Eur. Phys. J. E (2011) **34**: 102
DOI 10.1140/epje/i2011-11102-0

THE EUROPEAN PHYSICAL JOURNAL E

Regular Article

Field theory of fluctuations in glasses

S. Franz[1,a], G. Parisi[2], F. Ricci-Tersenghi[2], and T. Rizzo[2]

[1] Laboratoire de Physique Théorique et Modèles Statistiques, CNRS et Université Paris-Sud 11, UMR8626, Bât. 100, 91405 Orsay Cedex, France
[2] Dipartimento di Fisica, INFN - Sezione di Roma I, IPFC-CNR – UOS Roma Sapienza Università di Roma, P.le Aldo Moro 2, I-00185 Roma, Italy

Received 31 May 2011
Published online: 26 September 2011 –

Abstract. We develop a field-theoretical description of dynamical heterogeneities and fluctuations in supercooled liquids close to the (avoided) MCT singularity. Using quasi-equilibrium arguments, we eliminate time from the description and we completely characterize fluctuations in the beta regime. We identify different sources of fluctuations and show that the most relevant ones are associated to variations of "self-induced disorder" in the initial condition of the dynamics. It follows that heterogeneites can be described through a cubic field theory with an effective random field term. The phenomenon of perturbative dimensional reduction ensues, well known in random field problems, which implies an upper critical dimension of the theory equal to 8. We apply our theory to finite size scaling for mean-field systems and we test its prediction against numerical simulations.

1 Introduction

The heterogeneous character of glassy dynamics has been the object of extensive study in the last decade [1]. Experiments, simulations and theory converge to a description of supercooled liquids where, on approaching the glass transition, relaxation requires cooperative motions on high-mobility regions of increasing size and lifetime. An important theoretical step in the understanding of dynamical hetrogeneities has consisted in realizing that the current theory of glassy dynamics, the Mode Coupling Theory (MCT) [2,3], predicts a growing dynamical length as the Mode Coupling critical point is approached. This was first noted in the context of disordered mean-field systems where MCT is exact [4,5], and later confirmed with diagrammatic approaches to the dynamics of liquids [6]. In the resulting picture, the dynamical heterogeneities are captured by a time-dependent four-point correlation function, whose associated dynamical length diverges at the Mode Coupling critical point. As is well known, this divergence, which is genuine in mean field, is in real systems an artefactual consequence of MCT that neglects activated processes. The divergence is cut off as the MCT-dominated regime at high temperature crosses over to the barrier-dominated regime at low temperature. With this *caveat*, the MCT prediction of a pseudo-critical growth of dynamical correlations has been largely confirmed in numerical simulations [7] and experiments [8]. However, corrections to MCT are at work as soon as the mean-field approximation is not exact. Two kinds of corrections to MCT can be expected: those due to critical fluctuations which are not well described by mean-field theory, and those due to barrier jumping processes. Clarification of both kinds of fluctuations is necessary to have an accomplished theory of glassy dynamics. Unfortunately both kinds of phenomena are poorly understood.

The goal of this paper is to present an in-depth analysis of perturbation theory around MCT to study critical fluctuations. In doing that, we will neglect barrier jumping which is intrinsically of non-perturbative nature.

The Mode Coupling (MC) approximation describes an ergodicity breaking transition where a system prepared in an equilibrium initial condition remains confined in its vicinity. Correspondingly, two point-connected correlation functions develop an infinitely long plateau. This ergodicity breaking can be interpreted in the broader perspective of Random First Order Theory [9]. This theory predicts that within the approximations in which MCT is valid, at the dynamical transition the space of equilibrium configuration is partitioned in an exponentially large number of metastable states. Several aspects of dynamical freezing can then be conveniently studied through equilibrium techniques, introducing appropriate constraints in the Boltzmann-Gibbs measure [10–12]. The free energy as a function of the constraints provides a purely static field-theoretical description of the MC ergodicity breaking transition. This description has indeed been crucial to the first theoretical recognition of the growth of

[a] e-mail: silvio.franz@lptms.u-psud.fr

a dynamical susceptibility at a MC transition [4,5]. In this paper, we exploit this constrained equilibrium technique to devise a theory of critical fluctuations. The various dynamical characterization of fluctuations will be expressed in a *reparametrization invariant* form eliminating the time dependence in favor of a dependence on the average value of the (two point) correlation function itself[1]. This perspective allows enormous simplification with respect to the dynamical perturbation theory [15] which at present is limited to the Gaussian approximation. Previous studies have stressed the importance of the emerging reparametrization invariance at large times as a soft mode of fluctuations in [16–19] glassy dynamics. Our approach will allow us to give a universal description of these modes in the beta regime where dynamical correlation functions are close to their plateau value.

The main thesis of this paper is that reparametrization-invariant fluctuations for temperatures close to the mode coupling critical temperature T_d and values of the correlations close to the plateau value can be described in terms of a field theory of the kind

$$H[\phi|\delta\epsilon(x)] = \int \mathrm{d}x \frac{1}{2}(\nabla\phi(x))^2 + (\epsilon + \delta\epsilon(x))\phi(x) + g\phi^3(x), \quad (1)$$

where $\phi(x)$ is a local fluctuation of the overlap away from the plateau value, $\epsilon = T - T_d$ is the deviation from the critical temperature, g is a coupling constant and $\delta\epsilon(x)$ is an effective random temperature term, distributed with Gaussian statistics and delta correlated in space. The effective Hamiltonian (1) coincides with the one that describes the spinodal point of the Random Field Ising model (RFIM) [20]. We find that both problems are perturbatively in the same universality class. The random temperature term is the ultimate consequence of dynamic heterogeneity and is a formal expression of "self-induced disorder" sometimes advocated to describe structural glasses. The role of this term is crucial. Random field models are well-studied systems. It is well known that the random field changes the singular behavior of the theory. In particular in perturbation theory one finds the phenomenon of "dimensional reduction" which states that the singularities of the random model in dimension D are identical to the ones in the absence of disorder in dimension $D-2$. It follows that the upper critical dimension above which fluctuations can be expected to have a Gaussian nature is found to be eight rather then six, as could be expected from a pure ϕ^3 theory. It remains to find out if the Random Field Ising Model has a relevance for glassy dynamics beyond perturbation theory in the barrier-dominated regime.

The rest of the paper is organized as follows: in sect. 2 we analyze the sources of fluctuations in the systems and we define correlation functions sensitive to them. In sect. 3 we discuss constrained measures. We explain their use in the computation of correlation functions and how to obtain them from replica field theory. In sect. 4 we analyze the replica field theory close to the MC critical temperature and study the quadratic fluctuations. In sect. 5 we analyze deeply perturbation theory and we derive the effective field theory (1). Section 6 is devoted to finite size scaling in mean-field systems. The results of this last analysis are compared with numerical simulations in sect. 7. Finally we expose some concluding remarks in sect. 8.

A partial account of the theory and simulations exposed in this paper has been given in [21].

2 Measures of fluctuations

The theory exposed in this paper will be largely independent of the choice of systems. The main hypothesis we will make is that in some approximation a MC transition is present and we will study the generic behavior of fluctuations around it. Our theory applies equally well to describe critical fluctuations around the avoided MC transition in liquids as well as finite size scaling around MCT in mean-field spin models where the transition is sharp in the thermodynamic limit. With the former application in mind, in the following we will use the language of field theory. In our formulae finite size scaling in mean-field models can be obtained simply replacing all space integrations by an overall volume factor N.

For notational convenience, we will represent the systems in terms of spin variables fixed in space $S_i = \pm 1$, $i = 1, \ldots, N$. With this notation we can equally well describe genuine spin systems like spin glasses, but also liquid systems in a lattice gas representation where we divide the volume in small cells and use the spin —taking the two values ± 1— to represent the occupancy of the cells[2]. We will use as order parameter of freezing the correlation function, or overlap, among spin configurations. Given two configurations of the system S and S', we can define the local value of the overlap coarse-grained over some volumes v containing a large number of spins $|v| \gg 1$, $q_x(S, S') = |v|^{-1} \sum_{i \in v_x} S_i S'_i$. Different notions of correlations among configurations, *e.g.*, the one used in [22,23] lead to the same results, modulo a redefinition of the non-universal parameters appearing in (1). If we denote by $S(t)$ the configuration of the system at time t, the time-dependent correlation function can be written as $C(t,0) = \frac{1}{V}\int_V \mathrm{d}x q_x(S(0), S(t))$. The objects of our analysis will be the fluctuations in the global quantity $C(t,0)$ and the local quantities $q_x(S(0), S(t))$ as they can be studied through 4-point or higher-order correlation functions.

We would like to separate the contributions of different source of fluctuations of $C(t,0)$. For structural glasses we would like to distinguish fluctuations among different

[1] The terminology is mutated from asymptotic aging theory where time dependence is expressed through dependence on average correlations [13,14].

[2] Having in mind a monodisperse systems occupying a D-dimensional box of linear size L, we can divide the volume in $N = (L/a)^D$ cells of linear size a of the order of a fraction of the particle diameter. We then assign to each cell i the variable S_i which takes the value 1 if the center of a particle lies in the box and the value -1 otherwise.

trajectories that start from the same initial configuration from fluctuations due to changes in the initial condition itself. Recent numerical studies in supercooled liquids have emphasized the importance of this separation to study the influence of the structure in the development of dynamical heterogeneities [24–28]. For systems with quenched disorder, like *e.g.* spin glasses, one has a third source of fluctuations in the choice of the quenched interactions. In the following we assume without loss of generality the presence of some quenched disorder. If there is no disorder the respective averages are immaterial. We denote by $\langle\cdot\rangle$ the average over trajectories that start from the same initial condition. This was called iso-configurational average in [24–28]. The iso-configurational average can be the average over the initial velocities in the case of Newtonian dynamics or the average over thermal noise along the trajectories in the case of stochastic heat bath dynamics. The initial condition is denoted by $S(0) = S^0$ and will always be chosen as an equilibrium configuration in this paper. The corresponding average will be denoted by $[\![\cdot]\!]$. Finally averages over quenched disorder will be denoted by $\mathbb{E}(\cdot)$. A widely used measure of dynamical correlations is the 4-point correlation [29] $\chi_4(t) = N\mathbb{E}[\![\langle C(t)^2\rangle]\!] - (\mathbb{E}[\![\langle C(t)\rangle]\!])^2$. In order to quantify the contribution of each source of noise to this function, we use a decomposition of χ_4 in three different terms $\chi_4 = \chi_{th} + \chi_{het} + \chi_{dis}$ defined as [30]

$$\begin{aligned}
\frac{1}{N}\chi_{th}(t) &= \mathbb{E}([\![\langle C(t,0)^2\rangle]\!]) - \mathbb{E}([\![\langle C(t,0)\rangle^2]\!]),\\
\frac{1}{N}\chi_{het}(t) &= \mathbb{E}([\![\langle C(t,0)\rangle^2]\!]) - \mathbb{E}([\![\langle C(t,0)\rangle]\!]^2),\\
\frac{1}{N}\chi_{dis}(t) &= \mathbb{E}([\![\langle C(t,0)\rangle]\!]^2) - \mathbb{E}([\![\langle C(t,0)\rangle]\!])^2. \qquad (2)
\end{aligned}$$

These susceptibilities are the space integral of correlation functions that we will denote respectively $G_{th}(x,t)$, $G_{het}(x,t)$ and $G_{dis}(x,t)$. For example $G_{het}(x,t)$ can be expressed as

$$\begin{aligned}
G_{het}(x,t) = \mathbb{E}([\![&\langle q_x(S(0),S(t))\rangle\langle q_0(S(0),S(t))\rangle]\!]\\
&-[\![\langle q_x(S(0),S(t))\rangle]\!][\![\langle q_0(S(0),S(t))\rangle]\!]). \qquad (3)
\end{aligned}$$

In the case of liquids where quenched disorder is absent one has $\chi_{dis} = 0$ and

$$\begin{aligned}
\frac{1}{N}\chi_{th}(t) &= [\![\langle C(t,0)^2\rangle]\!] - [\![\langle C(t,0)\rangle^2]\!],\\
\frac{1}{N}\chi_{het}(t) &= [\![\langle C(t,0)\rangle^2]\!] - [\![\langle C(t,0)\rangle]\!]^2. \qquad (4)
\end{aligned}$$

In the following we will analyze the behavior of these three characterizations of fluctuations and predict their behavior for times such that the average correlation function $C_{av}(t) = \mathbb{E}([\![\langle C(t,0)\rangle]\!])$ is close to the plateau value C_p. As we will see in next section this can be achieved through quasi-equilibrium techniques at the price of eliminating time from the description. In the aforementioned time regime $C_{av}(t)$ is a decreasing function of time. We can express time dependence through the dependence on $C_{av}(t)$ itself. For any time-dependent quantity $O(t)$ we write $O(C) = O(t)|_{C_{av}(t)=C}$. All the time dependence is condensed in the dependence of $C_{av}(t)$ on time that we will leave unspecified.

3 Quasi-equilibrium in dynamics and constrained Boltzmann-Gibbs measures

In this section we discuss how to obtain information about equilibrium dynamics through the use of constrained equilibrium measures. This possibility relies in the phenomenon of time scale separation observed in glassy dynamics, where one can separate the degrees of freedom in fast and slow ones.

The dynamics of liquids close to the glass transition can be described as a slow process where the system passes from one metastable state to another. Time scale separation tells us that approximate equilibrium establishes in a given metastable state before a new state can be found. The equilibration time within a metastable state is identified by the time that the correlation function takes to stabilize to the plateau value C_p. In the beta regime metastable states are sampled in a quasi-ergodic fashion. On this time scale, the different four-point correlation functions introduced in the previous section can be then evaluated using constrained equilibrium measures that select the relevant metastable states. The set of constraints to be introduced should ensure that the relevant regions of configuration space in the restricted measure coincide with the ones sampled by the dynamics. The simplest possibility is to impose that in each region of space the overlap with a well-thermalized initial condition takes a fixed value. We will suppose that this specification of the local overlaps provides is a sufficient determination of the metastable states and assume that configurations that have a fixed overlap close to the plateau value with an equilibrium initial condition are sampled (almost) ergodically. This hypothesis —sometimes called separability [31, 32]— can be checked directly in mean-field spin glass systems and we believe it to be valid in supercooled liquids. In fact, we expect it to apply every time that glassiness is caused by the ruggedness of an energy landscape[3]. In the passage from dynamics to this quasi-equilibrium description we lose, of course, the possibility of studying the time dependence of the various quantities, that, as mentioned in the previous section, will be expressed instead as functions of the overlap in a *time reparametrization invariant* representation. In fig. 1 we illustrate how the four-point dynamical susceptibility of the spherical p-spin model [4,5] looks like if we operate this change of perspective.

Let us remark at this point that the use of a time-independent description of dynamical quantities has been widely used in the theory of aging [13,14], where reparameterization invariance emerges as an asymptotic continuous symmetry at large times. It was then proposed that this asymptotic zero mode could be used to characterize

[3] On the contrary, we do not expect it to apply in systems like kinetically constrained model, where the Hamiltonian is trivial. In this case the overlap does not give a sufficient determination of the metastable states [33].

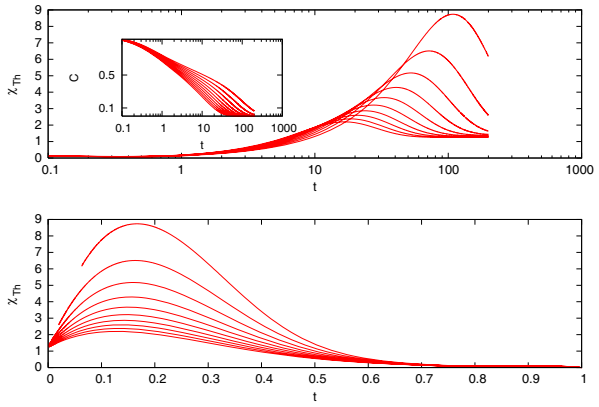

Fig. 1. The behavior of χ_{th} for the spherical p-spin model with $p = 3$. The curves are at temperatures $T = 0.665$, 0.68, 0.695, 0.71, 0.725, 0.74, 0.77, 0.785, 0.8, the critical temperature being $T_d = \sqrt{3/8} = 0.612$. Upper panel χ_{th} as a function of time. Inset: C as a function of time. Lower panel χ_{th} as a function of C.

fluctuations [16–19] in glassy states. Being based on symmetry considerations, this theory is very general, and concerns features of both the beta and the alpha regimes. Our theory, being based on quasi-equilibrium considerations, is less general and more specific: it will enable to give a detailed description of the beta regime, but it is limited to that. We will see, however, when discussing simulations, that looking at the data in reparametrization-invariant form is useful and inspiring also in the alpha regime.

In the rest of the paper we will concentrate on values of the temperature close to T_d, and ignore the possibility of an ideal glass transition at a lower temperature T_K.

We will concentrate on systems where either quenched disorder is absent, like in real liquids, or if disorder is present, its effect is weak and physical quantities can be evaluated to the leading order by the "annealed approximation". This is a stronger property than the usual self-averaging property of the free-energy and states that the *partition function* has small sample to sample fluctuations. Systems of this kind are often used to model structural glasses, and include, among others, fully connected p-spin models, spin models on diluted random graphs and finite range mean-field models in the Kac limit.

3.1 Effective potential: a Landau field-theoretical functional for the glass transition

According to the discussion of the previous section, we can select metastable states just choosing random equilibrium configurations S^0 and restricting the Boltzmann measure to configurations that do not differ too much from S^0. We achieve this fixing the local overlaps $q_x(S, S^0)$ to preassigned values p_x and defining a constrained measure [10–12]

$$\mu(S|S^0) = \frac{1}{Z[S^0, p_x]} e^{-\beta H(S)} \prod_x \delta(p_x - q_x(S, S^0)). \quad (5)$$

For systems that are separable in the sense specified in the previous section, the equilibrium metastable states are selected choosing in all points of space $p_x = C_p$, profiles that deviate from this shape allow to probe fluctuations.

The partition function $Z[S^0, p_x]$ is in fact directly related to the probability of the overlap profile

$$P(p_x|S^0) = e^{-\beta W(p_x, S^0)} = \frac{Z[S^0, p_x]}{Z}, \quad (6)$$

where Z is the unconstrained partition function. The large deviation functional $W(p_x, S^0)$ depends on the choice of the overlap profile but also on the choice of the reference configuration S^0 and on quenched noise in the case of disordered systems. In our formalism any dependence on S^0 quantifies the notion of "self-generated disorder" often advocated in the physics of structural glasses [34]. Previous studies have concentrated on the average value of W [10–12]. Depending on the nature of system under study, one can expect that the fluctuations of W with respect to S^0 and J are more or less strong. For example, in a fully connected model W is a function of a single global overlap parameter and self-averaging in the thermodynamic limit. Fluctuations decrease as powers of the system size. We will see, however, that fluctuations of the correlation functions and fluctuations in the potential can be related to each other. The entire probability distribution of W is therefore relevant to a complete description of glassy systems.

In fact, the present formalism allows in principle to compute the dynamic correlation functions that we have defined in the previous section in *reparametrization invariant form*. To this scope, we introduce the generating function of the overlap $\Gamma(h_x|S_0)$ defined by

$$e^{-\beta\Gamma(h_x, S^0)} = \int \mathcal{D}p_x \; e^{-\beta W(p_x, S^0) + \int \mathrm{d}x h_x p_x} \quad (7)$$

and define the static analogue of the correlations (3) in the presence of the field h_x as

$$\begin{aligned} G_{th}(x-y, h) &= \mathbb{E}([\![\langle p_x p_y\rangle - \langle p_x\rangle\langle p_y\rangle]\!]) = \\ &\quad \mathbb{E}([\![\langle p_x p_y\rangle_c]\!]), \\ G_{het}(x-y, h) &= \mathbb{E}([\![\langle p_x\rangle\langle p_y\rangle]\!] - [\![\langle p_x\rangle]\!][\![\langle p_y\rangle]\!]) = \\ &\quad \mathbb{E}([\![\langle p_x\rangle\langle p_y\rangle]\!]_c), \\ G_{dis}(x, h) &= \mathbb{E}([\![\langle p_x\rangle]\!][\![\langle p_y\rangle]\!]) - \mathbb{E}([\![\langle p_x\rangle]\!])\mathbb{E}([\![\langle p_y\rangle]\!]) = \\ &\quad \mathbb{E}([\![\langle p_x\rangle]\!][\![\langle p_y\rangle]\!])_c, \end{aligned} \quad (8)$$

where here we have denoted by $\langle\cdot\rangle$ the equilibrium average in the presence of h_x and with a subscript "c" the subtraction of the disconnected part. It is easy to check that the various correlations are related to the derivatives of the moments of the Γ functional according to

$$\begin{aligned} G_{th}(x-y, h) &= \mathbb{E}\left(\left[\!\!\left[\frac{\delta^2 \Gamma(h|S^0)}{\delta h_x \delta h_y} \right]\!\!\right] \right), \\ G_{het}(x, h) &= \mathbb{E}\left(\left[\!\!\left[\frac{\delta \Gamma(h|S^0)}{\delta h_x} \frac{\delta \Gamma(h|S^0)}{\delta h_y} \right]\!\!\right]_c \right), \\ G_{dis}(x, h) &= \mathbb{E}\left(\left[\!\!\left[\frac{\delta \Gamma(h|S^0)}{\delta h_x} \right]\!\!\right] \left[\!\!\left[\frac{\delta \Gamma(h|S^0)}{\delta h_y} \right]\!\!\right] \right)_c. \end{aligned} \quad (9)$$

If we fix the field h_x in such a way that $\mathbb{E}([\![\langle p_x \rangle]\!]) = q$ in all points of space, we get the correlation functions as a function of q. We need then a method to compute the cumulants of the functional W or equivalently the ones of Γ.

3.2 Effective potential and replicas

It is interesting to compute both the average of the potential $W(q_x, S^0)$ and its fluctuations. The replica method gives us a simple framework to undertake this task. As discussed many times [10–12], the average $W^{(1)}(p_x) = \mathbb{E}[\![W(p_x, S^0)]\!]$ can be computed considering

$$Z_m(p_x) = \mathbb{E}\left([\![Z[S^0, p_x]^m]\!]\right) = \mathbb{E}\left(\frac{1}{Z}\sum_{\{S^a\}_{a=0}^m} e^{-\beta\sum_{a=0}^m H(S^a)} \prod_{a=1}^m \prod_x \delta(p_x - q_x(S^a, S^0))\right) \tag{10}$$

valid for integer m, see footnote[4]. Notice that here the total number of replicas, which includes the reference configuration S_0 and the m copies of the constrained system, is $\mathbf{n} = m + 1$. The free-energy functional is obtained from an analytic continuation to $m = 0$, *i.e.* the total number of replicas $\mathbf{n}$ tends to 1.

$$W^{(1)}(p_x) = -T\frac{\partial Z_m(p_x)}{\partial m}\bigg|_{m=0} - F, \tag{11}$$

where F is the average unconstrained free energy of the system. Similarly one can get the second cumulants

$$W^{(2)}_{het}(p_x, p'_x) = \mathbb{E}([\![W(p_x, S^0)W(p'_x, S^0)]\!]_c) = T^2\,\frac{\partial^2 \log \mathbb{E}([\![Z[S^0, p_x]^{n_1} Z[S^0, p'_x]^{n_2}]\!])}{\partial n_1 \partial n_2}\bigg|_{n_1,n_2=0}, \tag{12}$$

$$W^{(2)}_{dis}(p_x, p'_x) = \mathbb{E}([\![W(p_x, S^0)]\!][\![W(p'_x, S^0)]\!])_c = T^2\,\frac{\partial^2 \log \mathbb{E}([\![Z[S^0, p_x]^{n_1}]\!][\![Z[S^0, p'_x]^{n_2}]\!])}{\partial n_1 \partial n_2}\bigg|_{n_1,n_2=0}, \tag{13}$$

where in the second equation we have exchanged the logarithm and the average over the disorder, thanks to the annealed approximation. Higher-order cumulants can be analogously obtained through more involved analytic continuations.

In order to unify the notation and treat all cases in parallel, it is convenient at this point to introduce the (formal) replica action $S[Q_x]$ for $\mathbf{n}$ replicas for fixed values of their mutual overlap $Q_{ab}(x)$ $(a, b = 1, \ldots, \mathbf{n})$ from

$$e^{-S[Q_x]} = \frac{1}{Z}\mathbb{E}\sum_{\{S^a\}_{a=1}^{\mathbf{n}}} e^{-\beta\sum_{a=1}^{\mathbf{n}} H(S^a)} \prod_{a,b=e}^{\mathbf{n}} \prod_x \delta(Q_{a,b}(x) - q_x(S^a, S^b)), \tag{14}$$

from which, integrating over some of the elements of the replica matrix and fixing some others, one can get the moments of W. For example one has that $W^{(1)}(p_x)$ can be computed by a replica action with $\mathbf{n} = m + 1$ replicas for $m \to 0$. Renumbering the replicas in a way that $a = 0, 1, \ldots, m$ one has

$$e^{-\beta m W^{(1)}(p_x)} = \int \mathcal{D}Q_{ab}(x) e^{-S[Q_x]} \prod_{a=1}^{\mathbf{m}} \delta(Q_{0,a}(x) - p(x)). \tag{15}$$

Analogously the correlation functions can be computed from a replica action with, respectively, $\mathbf{n} = n_1 + n_2 + 1$ and $\mathbf{n} = n_1 + n_2 + 2$ replicas for $n_1, n_2 \to 0$,

$$W^{(2)}_{het}(p_x, p'_x) = -T\,\frac{\partial}{\partial n_1 \partial n_2}\bigg|_{n_1,n_2=0} \times \log \int \mathcal{D}Q_{ab}(x) e^{-S[Q_x]} \prod_{a=1}^{n_1} \delta(Q_{0,a}(x) - p(x)) \times \prod_{a=n_1+1}^{n_1+n_2} \delta(Q_{0,a}(x) - p'(x)), \tag{16}$$

$$W^{(2)}_{dis}(p_x, p'_x) = -T\,\frac{\partial}{\partial n_1 \partial n_2}\bigg|_{n_1,n_2=0} \times \log \int \mathcal{D}Q_{ab}(x) e^{-S[Q_x]} \prod_{a=1}^{n_1} \delta(Q_{0,a}(x) - p(x)) \times \prod_{a=n_1+1}^{n_1+n_2} \delta(Q_{0',a}(x) - p'(x)), \tag{17}$$

where in the first case we have renumbered the replicas in a way that $a = 0, 1, \ldots, n_1 + n_2$ and in the second $a = 0, 0', 1, \ldots, n_1 + n_2$.

We would like at this point to remind that in disordered mean-field models there is a close relation between the Mode Coupling dynamical transition and the shape of $W^{(1)}(q)$, which in that case is a function of a single variable. In fact, the transition temperature T_d looks as a spinodal temperature for the potential $W^{(1)}$. This has a single minimum at low values of q at high temperatures, and develops a second minimum right at T_d for the value of the overlap $q = C_p$.

We argue that, in a separable system, where the measure (5) correctly samples metastable states, this is the generic situation. If metastability is found in some dynamical approximation, an approximation for statics with

[4] Thanks to the hypothesis of self-averageness of the partition function $1/Z \approx 1/\mathbb{E}(Z)$ the average over disorder in (10) does not require additional care.

the same physical content should lead to the appearance of a secondary minimum in the average effective potential corresponding to the constant profile $p_x = C_p$. Recent analysis of MCT as a Landau expansion [35] on one hand and reproduction of MCT results from replica Orstein-Zernike equations [36] on the other corroborate this point of view.

4 The replica action close to T_d

We enter now in the core of our analysis, and we study fluctuations for theories $S(Q)$ that at the level of homogeneous (*i.e.* space-independent) saddle point exhibit a dynamical phase transition at a temperature T_d. This is associated to the appearance of a horizontal inflection point at C_p in the effective potential $W^{(1)}(q)$, which becomes a minimum below T_d. As explained in detail in [10–12] (see also [37]) this inflection point is described by a $\mathbf{n} = 1$ replica-symmetric saddle point where $Q_{ab}(x) = Q^d_{ab} = C_p$ for all x and $a \neq b$. We wish to describe overlap fluctuations for T in the vicinity of T_d and p_x in the vicinity of C_p. A natural point of expansion of the action $S[Q]$ is the homogeneous saddle point just described. We can then expand in $\epsilon = T - T_d$ and the difference of $Q_{ab}(x)$ with C_p, $\phi_{ab}(x) = Q_{ab}(x) - C_p$ for $a \neq b$ and $\phi_{aa} = 0$. To the leading order one has a cubic theory

$$\begin{aligned} S[Q,T] = S_0[Q^d,T_d] &+ \int \mathrm{d}x \sum_{ab} \frac{\partial S[Q^d,T_d]}{\partial Q_{ab}(x)} \phi_{ab}(x) \\ &+ \sum_{ab} \frac{\partial^2 S[Q^d,T_d]}{\partial T \partial Q_{ab}(x)} \epsilon \phi_{ab}(x) \\ &+ \int \mathrm{d}x\, \mathrm{d}y \sum_{ab;cd} \phi_{ab}(x) M_{ab;cd}(x,y) \phi_{cd}(y) \\ &+ \int \mathrm{d}x\, \mathrm{d}y\, \mathrm{d}z \sum_{ab;cd;ef} \Omega_{ab;cd;ef}(x,y,z) \\ &\times \phi_{ab}(x)\phi_{cd}(y)\phi_{ef}(z). \end{aligned} \tag{18}$$

The second term vanishes for $\mathbf{n} = 1$, where Q^d is a solution to the saddle point equations. For generic $\mathbf{n}$, however, this is not the case, this will be a term of order $\mathbf{n} - 1$ that has to be kept in the expansion. To the lowest order in a gradient expansion and rescaling the variables to reabsorb superfluous constants, the action reads

$$\begin{aligned} S[Q] = S_0[Q^d] &+ \int \mathrm{d}x \sum_{ab} (A_{a,b} + \epsilon)\phi_{ab}(x) \\ &+ \frac{1}{2}\left(\sum_{ab} \nabla \phi_{ab}(x)\right)^2 + \frac{1}{2} \sum_{ab;cd} \phi_{ab}(x) M_{ab;cd} \phi_{cd}(x) \\ &+ \sum_{ab;cd;ef} \Omega_{ab;cd;ef} \phi_{ab}(x)\phi_{cd}(x)\phi_{ef}(x). \end{aligned} \tag{19}$$

Notice that the temperature couples linearly with $\phi_{ab}(x)$. This is due to the choice of the point of expansion as the inflection point at T_d. The components of A_{ab}, the mass operator $M_{ab;cd}$ and of the bare vertex $\Gamma_{ab;cd;ef}$ reflect the symmetry of the saddle point and should then depend only on the number indices that are equal or different. This immediately implies that the coefficients A_{ab} for $a \neq b$ should then be all equal, $A_{ab} = A(\mathbf{n}) \sim (\mathbf{n} - 1)A$, and that the quadratic form can be written as

$$\begin{aligned} S_2[\phi] = \frac{1}{2} \int \mathrm{d}x \Bigg(&\left(\sum_{ab} \nabla \phi_{ab}(x)\right)^2 + m_1 \sum_{ab} \phi^2_{ab} \\ &+ m_2 \sum_a \left(\sum_b \phi_{ab}\right)^2 + m_3 \left(\sum_{ab} \phi_{ab}\right)^2 \Bigg). \end{aligned} \tag{20}$$

The inclusion of all possible replica-symmetric cubic vertices gives rise to a cubic part [38]:

$$S_3(\phi_{ab}) = \int \mathrm{d}x \mathcal{L}^{(3)}, \tag{21}$$

$$\begin{aligned} \mathcal{L}^{(3)} = \frac{1}{6} \Bigg[&\omega_1 \sum_{abc} \phi_{ab}\phi_{bc}\phi_{ca} + \omega_2 \sum_{ab} \phi^3_{ab} \\ &+ \omega_3 \sum_{abc} \phi^2_{ab}\phi_{ac} + \omega_4 \sum_{abcd} \phi^2_{ab}\phi_{cd} \\ &+ \omega_5 \sum_{abcd} \phi_{ab}\phi_{ac}\phi_{bd} + \omega_6 \sum_{abcd} \phi_{ab}\phi_{ac}\phi_{ad} \\ &+ \omega_7 \sum_{abcde} \phi_{ac}\phi_{bc}\phi_{de} + \omega_8 \sum_{abcdef} \phi_{ab}\phi_{cd}\phi_{ef} \Bigg], \end{aligned} \tag{22}$$

however, we will show that only the first two terms are relevant for $\mathbf{n} \to 1$.

Notice that the average potential within the mean field is evaluated by a saddle point $\phi_{ab}(x) = \phi(x)$, which, inserted in (19) gives, to the lowest order in $\mathbf{n} - 1$,

$$\begin{aligned} W^{(1)}(\phi_x) = W(0) + \int \mathrm{d}x \frac{1}{2}(\nabla\phi)^2 + \epsilon\phi + \frac{1}{2}m_1\phi^2 + g\phi^3, \\ g = \frac{1}{6}(\omega_2 - \omega_1). \end{aligned} \tag{23}$$

Since by hypothesis we have developed around the horizontal inflection point for $\epsilon = 0$, we must have $m_1 = 0$.

Of course, different choices for the point of expansion are possible. In the region $T < T_d$ it is convenient to expand around the replica-symmetric saddle point $Q_{ab} = q_{EA}(T)$ at temperature T, *i.e.* around the point that describes the minimum of the average effective potential (23). This choice leads to an action like (19) where all terms linear in ϕ are absent. The factor m_1 is in this case non-zero and proportional to $\sqrt{-\epsilon}$. With this choice of the expansion point the average potential reads $W^{(1)}(\phi_x) = W(0) + \int \mathrm{d}x \frac{1}{2}(\nabla\phi)^2 + \frac{1}{2}m_1\phi^2 + g\phi^3$. In the following we will use both expansions, without introducing separate notations for the two.

Notice that we have written the expansion (19) for generic D-dimensional extended systems. However, as we will see in sect. 6, the same expansion can be used to describe finite-size corrections in fully connected disordered models and models on diluted random graphs. In that case the various overlaps are global quantities, the gradient term is absent and space integration is just substituted by an overall multiplication by the system volume N.

4.1 Quadratic free-energy fluctuations

In this section we discuss the correlation functions at the quadratic (one loop) level, neglecting the cubic part of the action. We study the fluctuations of the effective potential with respect to the choice of the initial configuration and the choice of quenched disorder. Our task is to compute $W^{(2)}_{het}$ and $W^{(2)}_{dis}$. To this scope, we observe that the one-loop order can be estimated as the saddle point of the n_1, n_2 derivative of $S[\phi]$ where some of the matrix elements are fixed. Let us start from $W^{(2)}_{het}(\phi, \phi')$. In this case we need to consider a saddle point of the action with $\mathbf{n} = 1 + n_1 + n_2$ replicas where the elements $\phi_{0,a}$ are fixed to $\phi_{0,a}(x) = \phi(x)$ for $a = 1, \ldots, n_1$, $\phi_{0,a}(x) = \phi'(x)$ for $a = n_1 + 1, \ldots, n_1 + n_2$. In the presence of such constraints, it is natural to look to a saddle point which is symmetric with respect to all the permutations that leave invariant the values of constraints, *i.e.* the group $S_{n_1} \times S_{n_2}$ of independent permutations of the first group and the second group of replicas among themselves. This is parametrized in terms of three fields $\psi(x)$, $\psi'(x)$ and $\psi_0(x)$ such that all the couples of replicas $a, b = 1, \ldots, n_1$ have the same overlap $\phi_{ab}(x) = \psi(x)$, all the couples of replicas $a, b = n_1 + 1, \ldots, n_1 + n_2$ have the same overlap $\phi_{ab}(x) = \psi'(x)$, and all the couples of replicas $a = 1, \ldots, n_1$ $b = n_1 + 1, \ldots, n_2$ have an overlap $\phi_{ab}(x) = \psi_0(x)$. Inserting this ansatz, one realizes that in the leading order in n_1, $n_2 \to 0$ the equations for ψ (respectively, ψ') are independent from ϕ' and ψ_0 (respectively, ϕ and ψ_0) and coincide with the ones that appear in the computation of $W^{(1)}$. In the limit of small ϵ the solution is simply $\psi = \phi$, $\psi' = \phi'$ and $\psi_0 = 0$, which gives

$$W^{(2)}_{het}[\phi_x, \phi'_x] = [\![W^2(0|S^0)]\!] + A \int \mathrm{d}x(\phi(x) + \phi'(x)) - (m_2 + m_3) \int \mathrm{d}x \phi(x)\phi'(x). \tag{24}$$

This formula has a clear interpretation: the effect of the heterogeneity in the reference configuration S^0 can be parametrized in terms of a space-dependent random free-energy shift $\alpha(x)$ and a random temperature $\delta\epsilon(x)$ which couples linearly to ϕ. This suggests that the potential $W(\phi|S^0)$ can be written as

$$W(\phi|S^0) = \int \mathrm{d}x \Big[\frac{1}{2}(\nabla\phi)^2 + (\epsilon + \delta\epsilon(x))\phi(x) + g\phi(x)^3 + \alpha(x) \Big]. \tag{25}$$

The free-energy shift and the random temperature are Gaussian mutually correlated fields with

$$[\![\alpha(x)\, \alpha(y)]\!] = [\![W^2(0|S^0)]\!]\delta(x - y)/V, \tag{26}$$

$$[\![\delta\epsilon(x)\, \delta\epsilon(y)]\!] = -(m_2 + m_3)\delta(x - y), \tag{27}$$

$$[\![\alpha(x)\, \delta\epsilon(y)]\!] = A\, \delta(x - y), \tag{28}$$

where the consistency of the theory requires $m_2 + m_3 \leq 0$. Formula (25) is the central result of our paper, derived here at the level of quadratic free-energy fluctuation. The effective field theory for the dynamic glass transition coincides with the one describing the spinodal point of the Random Field Ising model and therefore both problems are in the same universality class. It is well known that the leading singularities of random field theories in perturbation theory are given by the tree diagrams [39], or by the formal solution of the stochastic differential equation

$$-\Delta\phi + (\epsilon + \delta\epsilon(x)) + 3g\phi(x)^2 = 0. \tag{29}$$

In fact, even when this equation does not admit real solution, the complex solutions gives rise to a perturbation series for physical quantities with real coefficients. Though the analysis of the quadratic fluctuations give a strong hint about the validity of (25), one could doubt that the inclusion of the vertices in the theory modifies this result. As the matter of fact, in the next section we will analyze in depth the perturbation theory for $T < T_d$ and confirm (25) to all orders in perturbation theory.

Let us now briefly turn our attention to $W^{(2)}_{dis}$. In order to compute this quantity, one may follow a route similar to the computation of $W^{(2)}_{het}$. In this case, however, one can note that in annealed models the replicas 0 and 0′ have zero overlap, and an expansion around $q = C_p$ is not justified. Rather, one has that the mutual overlap between the replicas labeled $1, \ldots, n_1$ and the ones label-led $n_1 + 1, \ldots, n_1 + n_2$ should be put to zero. This leads to decoupling between the two groups of replicas and $W^{(2)}_{dis} = 0$ to the leading order. This is a remarkable result, showing that fluctuations due to disorder are much less important than fluctuations due to "self-generated disorder", seen here as heterogeneities in the reference configuration. We stress that the vanishing of $W^{(2)}_{dis}$ at the quadratic level is a consequence of the annealing hypothesis and certainly would not be true in systems where disorder fluctuations in the partition function have to be taken into account. In our view this absence of dependence on quenched disorder strongly supports the validity of long-range p-spin and similar models as good mean-field models for the structural glass transition.

Let us now exploit (24) to compute the overlap correlation functions (8). First of all we notice that at the tree level calculation the potential W and the generator Γ are related by

$$\Gamma_1[h] = \max_{q_x} W^{(1)}(q) - \int \mathrm{d}x h_x q_x. \tag{30}$$

This implies that the correlation function G_{th} at the one-loop level is given by

$$G_{th}(x - y) = \frac{\delta\Gamma_1[h]}{\delta h_x \delta h_y} = \left(\frac{\delta W^{(1)}[q]}{\delta q_x \delta q_y} \right)^{-1}. \tag{31}$$

We also notice that to the same accuracy

$$\Gamma^{(2)}_{het}[h,h'] = W^{(2)}_{het}(q,q'), \tag{32}$$

where q and q' are the maximizers of eq. (30) for field h and h', respectively. A simple computation of the derivative of $\Gamma^{(2)}_{het}$ shows that

$$G_{het}(x-y) = \frac{\delta\Gamma^{(2)}_{het}[h,h']}{\delta h_x \delta h'_y} = \int \mathrm{d}x'\mathrm{d}y' \frac{\delta W^{(2)}_{het}[q,q']}{\delta q_{x'}\delta q'_{y'}} G_{th}(x-x')G_{th}(y-y'). \tag{33}$$

The same computation for $G_{dis}(x-y)$ would yield the same formula with $W^{(2)}_{dis}$ at the place of $W^{(2)}_{het}$, but as we have remarked $W^{(2)}_{dis} = 0$ to the leading order. This implies that no singularity of G_{dis} can be detected in the quadratic theory. Beyond the Gaussian approximation, the singularity of G_{dis}, if any, should be weaker than the one of G_{th} and G_{het} and the possible presence of quenched disorder does not affect the universality class of the system. Equation (33) shows that, as soon as $\left(\frac{\delta W^{(2)}_{het}[q,q']}{\delta q_{x'}\delta q'_{y'}}\right)$ is non-zero, the order of the singularity in $G_{het}(x-y)$ is the double of the one of $G_{th}(x-y)$. Notice that $\left(\frac{\delta W^{(2)}_{het}[q,q']}{\delta q_{x'}\delta q'_{y'}}\right)$ is precisely equal to $[\![\delta\epsilon_x\delta\epsilon_y]\!] = -(m_2+m_3)\delta(x-y)$. We find the announced result that the largest source of fluctuations in the system comes from the heterogeneities in the initial condition. Its effect at the one-loop level is to double the singularity due to thermal fluctuations.

If we specify to the form (23) we find

$$\frac{\delta^2 W^{(1)}[q]}{\delta q_x \delta q_y} = \delta(x-y)\left(-\Delta + 6g\phi(x)\right). \tag{34}$$

Fixing now a constant overlap profile in space ϕ, we find that in momentum space

$$G_{th}(k,\phi) = \frac{1}{k^2+6g\phi}, \tag{35}$$

$$G_{het}(k,\phi) = -\frac{(m_2+m_3)}{(k^2+6g\phi)(k^2+6g\phi)}. \tag{36}$$

Both propagators are singular at $\phi = 0$ and $k = 0$, this corresponds to the divergence of the fluctuations at $\epsilon = 0$ and $q = C_p$. The fluctuations for $\epsilon \neq 0$ can be obtained inserting for ϕ a cut-off value of the order of the plateau $\phi_{EA} \sim \sqrt{|\epsilon|/g}$ and

$$G_{th}(k) = \frac{1}{k^2+\sqrt{g|\epsilon|}}, \tag{37}$$

$$G_{het}(k) = -\frac{(m_2+m_3)}{(k^2+\sqrt{g|\epsilon|})(k^2+\sqrt{g|\epsilon|})}. \tag{38}$$

Notice that, within the present Gaussian approximation, the intensity of critical temperature fluctuations $[\![\delta\epsilon_x\delta\epsilon_y]\!] = -(m_2+m_3)\delta(x-y)$ can be measured through the ρ ratio

$$\rho \equiv \frac{G_{het}(k,\phi)}{G_{th}(k,\phi)^2}, \tag{39}$$

at the critical point $\epsilon = 0$, $\phi = 0$. Beyond the Gaussian approximation, while (36) and (38) provide a clear indication that G_{het} is more singular than G_{th}, it is not clear to us if the relation $G_{het} \sim G^2_{th}$ continues to hold. This different scaling is an important result of our theory. Though our derivation is restricted to the beta regime, we will see in sect. 7 that numerical simulations show that a different scaling is also observed in the alpha regime.

5 Perturbation theory

We would like to confirm the description of fluctuations through the potential (25) by perturbation theory. In order to have a well-defined point of expansion in perturbation theory, we assume $T < T_d$ and we expand around the replica symmetric minimum of the action $Q_{ab}(x) = q_{EA}(T)$ for all a, b. Our starting point is then

$$S[\phi] = \int \mathrm{d}x \frac{1}{2}\left(\sum_{ab}(\nabla\phi_{ab})^2 + m_1\sum_{ab}\phi^2_{ab} + m_2\sum_a\left(\sum_b\phi_{ab}\right)^2 + m_3\left(\sum_{ab}\phi_{ab}\right)^2\right) + \mathcal{L}^{(3)}[\phi_x], \tag{40}$$

with $\mathcal{L}^{(3)}[\phi]$ given by (22) and $m_1 \sim \sqrt{-\epsilon}$.

5.1 The bare propagators

Let us now re-obtain the results on the 4-point functions of sect. 4.1 by studying the bare propagators of the replica field theory, as first derived in [40]. The analysis of a generic mass matrix with replica symmetric structure has been performed long ago by De Almeida and Thouless [41]. To analyze our case, we need to transpose their results to the case $\mathbf{n} \to 1$. There are in general three distinct eigenvalues of the quadratic form named longitudinal (L), replicon (R) and anomalous (A) in the current terminology. For future reference we remind that the longitudinal sector corresponds to fluctuations such that $\phi^L_{ab} = \phi$ independent of a, b ($a \neq b$), the replicon sector corresponds to fluctuation such that $\sum_b \phi^R_{ab}$ is vanishing for all a and the anomalous sector is the linear space of fluctuations orthogonal to the previous two. In terms of the parameters m_1, m_2 and m_3 of the quadratic form in (40), the eigenvalues for generic $\mathbf{n}$ read

$$\lambda_R(k) = k^2 + m_1, \tag{41}$$

$$\lambda_L(k) = k^2 + m_1 + (\mathbf{n}-1)(m_2+\mathbf{n}m_3), \tag{42}$$

$$\lambda_A(k) = k^2 + m_1 + \frac{(\mathbf{n}-2)}{2}m_2. \tag{43}$$

The replicon $\lambda_R(0) = m_1 \sim \sqrt{-\epsilon}$ is critical at the transition. Notice that for $\mathbf{n} = 1$ the longitudinal eigenvalue becomes degenerate with the replicon and therefore it also becomes critical at the transition.

It is already clear at this point that the replicon and longitudinal sections will give the most singular contribution to the perturbation theory. The propagator matrix of the theory in momentum space, $G^{(0)}_{ab;cd}(k) = (k^2 + M)^{-1}_{ab;cd}$ has the same replica symmetric structure as the mass matrix, so that we can write

$$G^{(0)}_{ab,cd}(k) = g_1 \frac{(\delta_{ac}\delta_{bd} + \delta_{ad}\delta_{bc})}{2} + g_2 \frac{(\delta_{ac} + \delta_{ad} + \delta_{bc} + \delta_{bd})}{4} + g_3. \quad (44)$$

The coefficients g_1, g_2 and g_3 can be easily expressed in terms of the eigenvalues of the mass matrix, or in terms of the m parameters, the result for $\mathbf{n} = 1$ is

$$g_1 = \frac{1}{k^2 + m_1}, \quad (45)$$

$$g_2 = -\frac{m_2}{m_2/2 + k^2 + m_1} \frac{1}{k^2 + m_1} \sim \frac{1}{k^2 + m_1}, \quad (46)$$

$$g_3 = \frac{1}{k^2 + m_1} \left[\frac{-(m_2 + m_3)}{k^2 + m_1} + \frac{m_2}{m_2/2 + k^2 + m_1} \right]. \quad (47)$$

The replica formalism naturally embeds the distinction among different sources of fluctuations discussed in sect. 2 and allows to easily compute the propagators G_{th} and G_{het} of sect. 2 to the one-loop order. This can be done noticing that $\mathbb{E}([\![\langle\phi^2\rangle]\!]) = G_{ab,ab}$, $\mathbb{E}([\![\langle\phi\rangle^2]\!]) = G_{ab,ac}$, where all the replica indices are different one from the other

$$G_{th}(k) = G_{ab;ab} - G_{ab;ac} = g_1 - g_2 \sim \frac{1}{k^2 + m_1}, \quad (48)$$

$$G_{het}(k) = G_{ab;ac} = g_2 + g_3 \sim \frac{-(m_2 + m_3)}{(k^2 + m_1)^2}. \quad (49)$$

Coherently with the results of sect. 4.1 the singularity of G_{th} is a single pole while the one of G_{het} is a double pole. Within the replica formalism the origin of the double singularity stems from the degeneracy of the replicon and the longitudinal eigenvalues for $\mathbf{n} \to 1$, which both become critical at the transition.

5.2 A perturbative derivation of the stochastic equation

We would like now to analyze the complete theory and show that the leading singularities in perturbation theory coincide with the one given by the stochastic differential equation (29). The analysis we perform is similar to the analysis of random field models as originally put forward by Parisi and Sourlas [39]. This is based on dimensional evaluation of the various vertices of the theory for $\mathbf{n} \to 1$ exploiting a change of basis that generalizes the one suggested by Cardy in [42,43] for the RFIM. We note first of all that the leading singularities come from the replicon and longitudinal modes, that become critical at the transition. We therefore concentrate on these modes, for which the matrix ϕ_{ab} is such that $\sum_b \phi_{ab}$ is independent of a. Symmetric matrices with this property form a linear space of dimension $(\mathbf{n}-1)(\mathbf{n}-2)/2$. We now describe fluctuation in a different basis separating the fluctuating replica matrix in replica symmetric part, independent of the indices, plus a replica symmetry breaking fluctuations and write, for $a \neq b$ and all points in space,

$$\phi_{ab} = \phi - \frac{1}{2}\omega + U_{ab}\,\omega + \chi_{ab}, \quad (50)$$

$$\sum_b \chi_{ab} = 0 \quad \forall\ a, \quad (51)$$

$$\sum_{a,b} \chi_{ab} U_{ab} = 0, \quad (52)$$

where we have defined U_{ab} as a constant block matrix which has all elements equal to zero except the ones for which $b = a + 1$ and a is odd or $b = a - 1$ and a is even, *i.e.*

$$U_{ab} = \begin{cases} 1, & \text{if} \quad b = a - (-1)^a, \\ 0, & \text{otherwise.} \end{cases} \quad (53)$$

In this new basis we will be able, on the one hand, to perform the $\mathbf{n} \to 1$ limit directly in the action and, on the other hand, to evaluate the scaling dimension of the different terms in the action in order to keep only the most singular ones. Notice that the "vectors" ϕ_{ab} defined by (52) span the longitudinal and replicon sector and that the matrices χ_{ab} verifying the above relations form a linear space of dimension $(\mathbf{n}-1)(\mathbf{n}-2)/2 - 2$. We observe now that

$$\sum_b \phi_{ab} = \omega + (\mathbf{n} - 1)\left(\phi - \frac{1}{2}\omega\right), \quad (54)$$

$$\sum_{a,b} \phi^2_{ab} = \mathbf{n} 2\omega\phi + \sum_{a,b} \chi^2_{ab} + \mathbf{n}(\mathbf{n}-1)\left(\phi - \frac{\omega}{2}\right)^2. \quad (55)$$

Neglecting all the terms that vanish in the $\mathbf{n} \to 1$ limit, the quadratic part of the action reads

$$S_2 = \int \mathrm{d}x \left(2(\nabla\phi)(\nabla\omega) + \sum_{ab} (\nabla\chi_{ab})^2 + m_1 \left(\phi\omega + \frac{1}{2}\sum_{a,b} \chi^2_{ab} \right) + \frac{1}{2}(m_2 + m_3)\omega^2 \right). \quad (56)$$

Let us now study the m_1-mass dimensions D_ϕ, D_ω and D_χ of the fields ϕ, ω and χ_{ab}. As usual we impose that all terms in S_2 have the same dimension. We consider the case in which m_2 and m_3 remain finite at the transition, while $m_1 \to 0$. In this case we can write

$$D_\omega = D_\phi + 1, \quad (57)$$

$$D_\chi = D_\phi + \frac{1}{2}. \quad (58)$$

Let us now analyze the vertices. Expressed in the new variables the first four vertices of (22) read

$$\sum_{a,b,c}\phi_{ab}\phi_{bc}\phi_{ca} = (\mathbf{n}-1)(\mathbf{n}-2)\left(\phi-\frac{\omega}{2}\right)^3 -3\phi\sum_{ab}\chi_{ab}^2+3\mathbf{n}(\mathbf{n}-2)\omega\phi^2+\mathrm{Tr}\,\chi^3 +\omega\,\mathrm{Tr}\,\chi^2 U-\frac{3}{2}\omega\sum_{ab}\chi_{ab}^2 +3\phi\omega^2\mathbf{n}(\mathbf{n}-2)+\omega^3\mathbf{n}\left(\frac{3}{4}\mathbf{n}-2\right), \quad (59)$$

$$\sum_{ab}\phi_{ab}^3 = \mathbf{n}(\mathbf{n}-1)\left(\phi-\frac{\omega}{2}\right)^3+3\phi\sum_{ab}\chi_{ab}^2 +3\mathbf{n}\omega\phi^2+\sum_{ab}\chi_{ab}^3+3\omega\sum_{ab}\chi_{ab}^2U_{ab} -\frac{3}{2}\omega\sum_{ab}\chi_{ab}^2+6\mathbf{n}\omega^2\phi+\mathbf{n}\frac{\omega^3}{4}, \quad (60)$$

$$\sum_{a,b,c}\phi_{ab}^2\phi_{ac} = \left(\omega+(\mathbf{n}-1)\left(\phi-\frac{1}{2}\omega\right)\right)\left(\mathbf{n}2\omega\phi +\sum_{a,b}\chi_{ab}^2+\mathbf{n}(\mathbf{n}-1)\left(\phi+\frac{\omega}{2}\right)^2\right), \quad (61)$$

$$\sum_{a,b,c,d}\phi_{ab}^2\phi_{cd} = n\sum_{a,b,c}\phi_{ab}^2\phi_{ac}, \quad (62)$$

all the other combinations that appear in S_3, *i.e.* vertices 5 to 8, give just rise to terms proportional to ω^3 plus terms that vanish for $\mathbf{n}\to 1$. Notice that all the terms proportional to ϕ^3 vanish for $\mathbf{n}\to 1$. In the new basis, the mass dimensions of the vertices that survive for $\mathbf{n}\to 1$ are

$$\omega\phi^2, \qquad \phi\sum_{ab}\chi_{ab}^2\to 3D_\phi+1, \quad (63)$$

$$\sum_{ab}\chi_{ab}^3, \qquad \mathrm{Tr}\,\chi^3\to 3D_\phi+\frac{3}{2}, \quad (64)$$

$$\omega\sum\chi_{ab}^2, \qquad \omega\,\mathrm{Tr}\,\chi^2U, \qquad \omega^2\phi\to 3D_\phi+2, \quad (65)$$

$$\omega^3\to 3D_\phi+3. \quad (66)$$

The leading singular behavior in perturbation theory of the theory for $m_1\to 0$ is dictated by the first two vertices (63), which are the ones of lower dimension. Neglecting therefore the subleading vertices, we find that we can write the action as

$$S=\int \mathrm{d}x\frac{1}{2}(m_2+m_3)\omega^2+\omega\left(-\Delta\phi+m_1\phi+3g\phi^2\right) +\frac{1}{2}\sum_{a,b}\chi_{ab}\left(-\Delta+m_1+6g\phi\right)\chi_{ab}, \quad (67)$$

where $g=\omega_2-\omega_1$. We observe that the matrix field $\chi_{ab}(x)$ has $(\mathbf{n}-1)(\mathbf{n}-2)/2-2\to -2$ independent components and becomes equivalent to a couple of anticommuting fermion fields $\chi(x)$ and $\bar\chi(x)$ for $\mathbf{n}\to 1$. Equivalently, we can observe that the explicitly integration over the χ_{ab} fields gives rise to

$$\det\left(-\Delta+m_1+6g\phi(x)\right)^{1-(\mathbf{n}-1)(\mathbf{n}-2)/4}\underset{\mathbf{n}\to 1}{\longrightarrow} \det\left(-\Delta+m_1+6g\phi(x)\right). \quad (68)$$

We finally recognize in the action (67) a Parisi-Sourlas supersymmetric theory associated with the stochastic equation

$$-\Delta\phi(x)+m_1\phi(x)+3g\phi(x)^2+\delta\epsilon(x)=0, \quad (69)$$

where $\delta\epsilon(x)$ is a Gaussian field with variance

$$[\![\delta\epsilon(x)\delta\epsilon(y)]\!]=-(m_2+m_3)\delta(x-y). \quad (70)$$

If we impose that all the terms in the action have the same scaling dimension, we find $D_\phi=1$ and in D spatial dimension the action has dimension $-\frac{D}{2}+4$. It is well known that Parisi-Sourlas actions present a supersymmetry that leads to the phenomenon of dimensional reduction. The perturbation theory of the system in a random field in dimension D coincides with the one of a pure system in dimension $D-2$. Coherently the upper critical dimension of the theory is promoted to 8 from the value 6 of the pure ϕ^3 theory.

From the (formal) solution of eq. (69) $\phi(x)$, we can obtain the correlation functions G_{th} and G_{het} through linear response theory, using (70)

$$G_{th}(x-y)=[\![\frac{\delta\phi(x)}{\delta\epsilon(y)}]\!]=\frac{-1}{m_2+m_3}[\![\phi(x)\times\delta\epsilon(y)]\!],$$
$$G_{het}(x-y)=[\![\phi(x)\phi(y)]\!]_c. \quad (71)$$

The derivation leading to (67), (68), (69), (70) is valid within the perturbation theory. Its expression should be considered as a formal writing valid within the perturbative context. In fact, due to the cubic nature of the potential, eq. (69) admits a real solution only if $\delta\epsilon(x)$ is sufficiently small in absolute value in all points of space. For a Gaussian field $\delta\epsilon(x)$ this condition is violated with probability one in an infinite space. The consequence of that is that the perturbation series should be divergent. In fact, the perturbation theory is formally identical to the one of branched polymers considered in [44], with the crucial difference that in polymer's case the coupling constant g is purely imaginary [45], while in the present case it is real. In the branched polymer case the perturbative series is resummable thanks to the fact that its terms have alternating signs. Here, all terms have the same sign, the resulting series is badly divergent and it seems hardly resummable. Recent work has used "Exact Renormalization Group" [46] methods to compute the exponents of the thermodynamic transition of the RFIM [47,48]. It is not clear to us if these methods can be useful to study the spinodal point.

A fast way of realizing that perturbation theory should be divergent comes from considering eq. (69) in the homogeneous limit of space-independent quantities. As we will

describe in the next section, this allows to describe finite size scaling in mean-field models. In this case the equation reads

$$m_1\phi + 3g\phi^2 + \delta\epsilon = 0, \tag{72}$$

where now the variance of $\delta\epsilon$ is given by

$$[\![\delta\epsilon\delta\epsilon]\!] = -\frac{(m_2+m_3)}{N}\,. \tag{73}$$

The correlation function G_{het} can be formally evaluated from the solution $\phi^* = \frac{-m_1+\sqrt{m_1^2-12g\delta\epsilon}}{6g}$ as

$$G_{het}(\epsilon,N) = \frac{1}{N}\left([\![(\phi^*)^2]\!] - [\![\phi^*]\!]^2\right). \tag{74}$$

This correlation can be evaluated in an expansion in $\delta\epsilon$, giving rise to well-defined series with real coefficients. However it is clear that the series cannot be convergent, as the averages in (74) receive an imaginary contribution from the square root in the region $\delta\epsilon > m_1^2/12g$.

Putting these problems of convergence aside, one can ask if, for typical disorder realization $\delta\epsilon(x)$, the stochastic equation (69) could be used beyond perturbation theory in a description of the barrier jumping processes in a reparametrization-invariant way. While we do not have a definite answer in general, we will discuss the consequence of this hypothesis for mean-field finite size scaling in the next section.

6 Finite size scaling around mean field

6.1 The beta region

The theory that we have developed can be easily generalized to describe finite size scaling in mean-field systems which have a genuine MC dynamical phase transition in the thermodynamic limit. These include disordered spin models like p-spin and Potts defined on fully connected or finitely connected random graphs, and problems that appear in computer science and information theory like the K-SAT or XOR-SAT problem or error correcting codes. For large but finite sizes N the dynamical transition is cut off. Finite size scaling should describe the crossover to criticality for $N\to\infty$ and $\epsilon\to 0$.

A phenomenological theory of dynamic finite size scaling for disordered mean-field models has been first proposed in [49]. In order to interpret numerical results, in ref. [49] a sample-dependent critical temperature was assumed and the Harris criterion was used to derive scaling variables and exponents. Our results, using a fundamental theoretical description, confirm and rationalize that analysis as far as reparametrization invariant quantities are concerned. As discussed above, the origin of the random temperature term is in our theory a consequence of dynamical heterogeneity rather than of quenched disorder.

To analyze mean-field finite size scaling, we follow the lines drawn in the previous sections, except that in this case overlaps do not display space, that is we use observables integrated over the whole system. The relevant replica action is identical to the one discussed in sect. 4 without the gradient term and with space integration substituted by an overall volume factor N.

Repeating the analysis of the replica action that led to (25) and (69) in this case, we get a description in terms of a single variable effective potential $W(\phi|S_0)$ describing the total overlap fluctuations around the plateau value, $\phi = q - C_p$

$$W(\phi|S^0) = W(0|S^0) + N\left([\epsilon+\delta\epsilon]\phi + g\phi^3 + \alpha\right), \tag{75}$$

where in this case both $\delta\epsilon$ and α are Gaussian covaring variables of order $1/\sqrt{N}$. In terms of the parameter of the replica field theory, $g = \frac{1}{6}(\omega_2-\omega_1)$, $[\![\alpha\alpha]\!] = \frac{1}{N}[\![W^2(0|S_0)]\!]$, $[\![\alpha\delta\epsilon]\!] = \frac{1}{N}A$, $[\![\delta\epsilon^2]\!] = -\frac{1}{N}(m_2+m_3)$. Correspondingly we get the Parisi-Sourlas action

$$S = N\left(\frac{m_2+m_3}{2}\omega^2 + \omega(\epsilon+3g\phi^2) + \chi 6g\phi\bar{\chi}\right). \tag{76}$$

From formula (76) the properties of finite size scaling readily follow from dimensional analysis. We are interested in the behavior of the various observables in the critical crossover region for $N\to\infty$ and $\epsilon\to 0$. This is the region of variables such that all terms in the action are of order one, namely $\phi\sim\sqrt{|\epsilon|}$, $\omega\sim\epsilon\sim N^{-1/2}$ and χ, $\bar{\chi}\sim N^{-3/8}$. This allows to identify as scaling variables $x=\phi N^{1/4}$ and $y=\epsilon N^{1/2}$ in quantities that depend on size, temperature and overlap. Mutating the results of sect. 4.1 on the behavior of quadratic fluctuations, we find that, for $\phi\to 0$ and $N\to\infty$, $\chi_{th}\sim\frac{1}{\sqrt{|\epsilon|}}$ and $\chi_{het}\sim\frac{1}{|\epsilon|}$. Trading N for ϵ, this implies that in the crossover region

$$\chi_{th}(\phi,\epsilon,N) = N^{1/4} f_{th}(\phi N^{1/4}, \epsilon N^{1/2}), \tag{77}$$

$$\chi_{het}(\phi,\epsilon,N) = N^{1/2} f_{het}(\phi N^{1/4}, \epsilon N^{1/2}). \tag{78}$$

In order to match the singularities for $N\to\infty$, the scaling functions $f_{th}(x,y)$ and $f_{het}(x,y)$ verify $f_{th}(0,y)\sim\frac{1}{\sqrt{y}}$, $f_{th}(x,0)\sim\frac{1}{x}$ and $f_{het}(0,y)\sim\frac{1}{y}$, $f_{het}(x,0)\sim\frac{1}{x^2}$ for $x\to+\infty$ or $y\to+\infty$, while a finite limit should be expected at small values of the two arguments.

It is interesting to study the behavior of the ratio $\rho = \chi_{het}/\chi_{th}^2$ in the scaling window. In the $N\to\infty$ limit this ratio can be related to the variance of the random field by the relation: $\lim_{\phi\to 0}\lim_{N\to\infty}\rho(\epsilon=0,\phi,N) = -(m_2+m_3)$ where the limits should be taken in the order. In the scaling window, on the other hand, $\rho(\epsilon,\phi,N) = f_{het}(x,y)/f_{th}(x,y)^2$. Consistency requires that $\lim_{y\to\infty} f_{het}(0,y)/f_{th}(0,y)^2 = -(m_1+m_2)$. As we have observed in the previous section, the perturbative series of the scaling functions are badly divergent and can hardly be computed analytically. Thus, this is as far as we can go from the perturbative analysis of (76). Numerical verification of the scaling forms (78) will be the object of the next section.

6.2 The alpha regime: some conjectures

In the deep alpha regime, where $\phi < 0$ is of order one in absolute value, quasi-equilibrium in the sense we were using so far does not hold, the configuration space with average correlation $C < C_p$ is not sampled ergodically and our theory does not apply. However, this does not make it less interesting to look at the time reparameterization-invariant part of the fluctuations and, on the contrary, calls for new theoretical ideas to be developed. One can hope that finite size scaling of mean-field models is a simple enough setting to put forward hypotheses to be tested in the general case. This section will be then by nature much more conjectural and qualitative than the previous ones.

In order to understand finite size scaling in the alpha region, we can conjecture continuity with the behavior in the scaling regime $\phi \sim N^{-1/4}$ and quote the results of the analysis of dynamic Gaussian fluctuation theory developed in [15]. This predicts that the peak χ_4^* of the dynamic susceptibility as a function of time lies deep in the alpha region and scales as $\frac{1}{\epsilon^2}$, see footnote[5]. If we assume that this scaling holds in the whole regime $C < C_p$, we can match the form (78) if we suppose that the function $f_{het}(x, y)$ behaves quadratically for large negative values of x. In this way $\chi_{het}(\phi, \epsilon, N) = N^{1/2} f_{het}(\phi N^{1/4}, \epsilon N^{1/2}) \simeq N\phi^2 g_{het}(\epsilon N^{1/2})$ for $-\phi N^{1/4} \gg 1$, where the function $g_{het}(y)$ should behave as y^{-2} for large argument and take a finite value for $y = 0$. This implies that in the alpha region one has that for $\epsilon = 0$, $\chi_{het} = O(N)$. If we also assume that $f_{th}(x, y)$ behaves quadratically for large negative x, we get $\chi_{th}(\phi, \epsilon, N) = N^{1/4} f_{th}(\phi N^{1/4}, \epsilon N^{1/2}) \simeq N^{3/4}\phi^2 g_{th}(\epsilon N^{1/2})$; which implies a $N^{3/4}$ scaling of χ_{th} for $\epsilon = 0$ and a behavior as $\epsilon^{-3/4}$ for small positive ϵ and $N \to \infty$. A linear behavior $f_{th}(x, y) = x h_{th}(y)$ would give $\chi_{th} \sim N^{1/2}$ for $\epsilon = 0$ and $\chi_{th} \sim \epsilon^{-1}$ for small ϵ and $N \to \infty$.

Away from criticality, a simple dynamical scenario can be conjectured for the alpha relaxation in the barrier-dominated region $\epsilon < 0$ and $N \to \infty$. We make a crucial assumption that in a first approximation in the region $\epsilon \leq 0$, the reparameterization-invariant fluctuations in the alpha region are equivalent to the ones of a simple barrier jumping process, as described, for example, by the Langevin equation

$$\frac{\mathrm{d}q}{\mathrm{d}s} = -W'(q|S^0) + \eta \tag{79}$$

in the weak noise limit $\eta \ll 1$. The waiting time before a jump is a random variable whose typical values are much larger than the time required to pass from C_p to 0 when the jump occurs. This leads to a bistable behavior that naturally gives rise to $O(1)$ fluctuations of the overlap. At any given instant of time one has just a small probability of finding $C(t)$ to be different from C_p or 0. Neglecting this probability we find a general form of the total susceptibility $\chi_4(q)$, which is independent of the barrier. Suppose now to fix time in a way that for each value of the system size $C_{av} = [\![\langle C \rangle]\!]$. The histogram of C for different trajectories and initial conditions is approximately given by

$$P(C|C_{av}) = \frac{C_{av}}{C_p}\delta(C - C_p) + \left(1 - \frac{C_{av}}{C_p}\right)\delta(C). \tag{80}$$

The direct computation of $\chi_4(C_{av})$ using (80) leads to the simple expression

$$\chi_4(C_{av})/N = C_{av}(C_p - C_{av}). \tag{81}$$

This form is independent of the barrier and valid in the whole region $T < T_d$. As we will see in the next section, these hypotheses provide a good (but still not perfect) description of numerical results even at $\epsilon = 0$. Notice that in deriving (81) we have just used bistability and not the detailed Langevin equation (79).

One can then try to use similar ideas to describe the alpha relaxation in finite-dimensional systems. For example, numerical simulations in [51] suggest that bistability as described by (80) approximately holds for the probability of the local overlap $q_x(t)$ coarse grained on scales smaller than the correlation length. It would be then tempting to write an equation analogous to (79), with an additional Laplacian term to describe the decay of the overlap. Unfortunately the phenomenology of such an equation [52], which describes the competition between different phases in the presence of disorder, is rather distant from the one of supercooled liquids. In particular such an equation would predict nucleation events as they could be expected in liquids, but also the fast growth of supercritical nuclei of low overlap that cannot be expected.

7 Simulations

In order to test the theoretical predictions derived above, we have simulated the 3-spin model on a random regular graph, *i.e.* a random graph of fixed connectivity z. This model involves N Ising spins $S_i = \pm 1$ interacting through the Hamiltonian

$$H[S] = -\sum_{\mu=1}^{M} J_\mu S_{i_1^\mu} S_{i_2^\mu} S_{i_3^\mu}, \tag{82}$$

where the indices $i_1^\mu, i_2^\mu, i_3^\mu$ are chosen at random in such a way that each spin participates exactly to $z = 3M/N$ interactions and the couplings J_μ are independent random variables taking values ± 1, with $\mathbb{P}(J_\mu = 1) = r$. The properties of the model in thermodynamic limit are well known [53]. In particular if $z \geq 4$ the model exhibits a MC-like dynamical phase transition at temperature T_d and a Kauzmann ideal glass transition at a lower temperature T_k; both transition temperatures depend on z, but not on

[5] In [15] this behavior was found to hold only for conservative dynamics. Later analysis showed that the same behavior also holds generically even in the absence of dynamically conserved quantities [50].

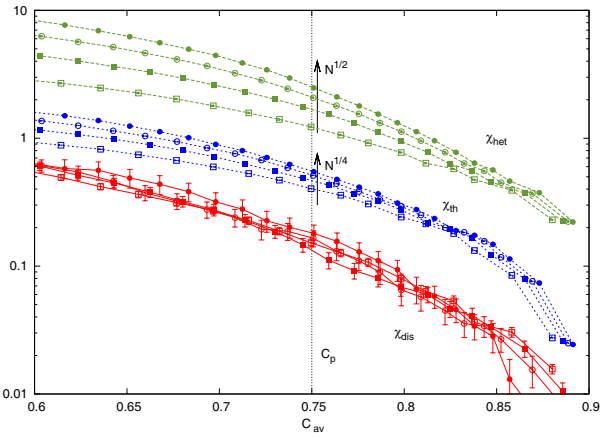

Fig. 2. Three different susceptibilities χ_{dis}, χ_{th} and χ_{het} (from bottom to top) *versus* average correlation C_{av} for the 3-spin symmetric model. The χ_{th} data have been divided by a factor 3 in order to avoid data overlap. The vertical line marks the analytical value of $C_p = 0.75$. System sizes are $N = 60, 90, 120, 150$ (from bottom to top for each susceptibility).

r. In fact it is well known that the thermodynamic and dynamic properties of the model are independent of the choice of r for temperatures $T > T_k$. In this range of temperature the model is annealed: that is, denoting Z_J the partition function for a given disorder realization J, one has that $\lim_{N\to\infty} \frac{1}{N}\mathbb{E}\log Z_J = \lim_{N\to\infty} \frac{1}{N}\log \mathbb{E}Z_J$. This property is true in particular for the *symmetric model* with $r = 1/2$ and for the *gauged model* defined by the Nishimori condition $r = (1 - e^{-2\beta})^{-1}$ [54]. Although the two versions of the model (the symmetric and the gauged one) have the same thermodynamical behavior for $T > T_k$, they may show very different finite size effects. In the following we study both versions.

We choose to simulate the case $z = 8$. The analytic solution to the model [53] predicts, in the thermodynamic limit, a dynamical temperature $T_d = 1.3420(5)$ and the plateau value at T_d equal to $C_p = 0.750(5)$. All the results shown in the following have been obtained at the dynamical critical temperature T_d.

7.1 Simulations in the beta regime

We start by showing results obtained with the symmetric model ($r = 1/2$). We have simulated at the dynamical critical temperature T_d systems of size ranging from $N = 60$ to $N = 150$, with a number of samples N_S such that $N \times N_S = 1.8 \cdot 10^6$. For each sample, we have obtained 2 independent equilibrium configurations (with the use of the parallel tempering algorithm), and, from each of these, we have evolved 2 independent trajectories with different thermal noises: this allows us to compute all the three different fluctuations χ_{dis}, χ_{th} and χ_{het} (see below the detailed explanation for the gauged model).

In fig. 2 we plot these three susceptibilities χ_{dis}, χ_{th} and χ_{het} measured in the symmetric model ($r = 1/2$) for sizes $N = 60, 90, 120, 150$. In the symmetric model, we cannot study larger sizes due to the very large thermalization times. Nonetheless, even for these relatively small sizes, we can clearly see the very different size dependence of the susceptibilities at the critical point, $C_{av} = C_p$. As expected from the discussion in sect. 4.1, χ_{dis} is practically size independent within error bars, while χ_{th} and χ_{het} are well compatible with the predicted scaling laws, $N^{1/4}$ and $N^{1/2}$, respectively. Unfortunately data are plagued by severe finite size effects even in the beta region, $C_{av} > C_p$.

In order to reach a clearer conclusion about the scaling laws in the beta regime and at the critical point, we need to study larger systems and this is the reason for using the gauged model, where an equilibrium configuration can be generated without the long thermalization process [55–57]. Indeed, on the Nishimori line, for a given interaction graph, one can first choose an arbitrary spin configuration S^0, and then fix the coupling J_μ such that S^0 is an equilibrium configuration. This can be done by choosing the couplings as independent random variables taking values ± 1 with the following probability:

$$\mathbb{P}(J_\mu|S^0) = \frac{\exp(-\beta J_\mu S^0_{i_1^\mu} S^0_{i_2^\mu} S^0_{i_3^\mu})}{2\cosh(\beta)}\,. \tag{83}$$

Since S^0 can be arbitrary, it is customary to set $S^0_i = 1$ for all i, a convention that we will adopt in the following. As a drawback of the method we note that, since we generate at the same time initial configuration and quenched couplings, we cannot disentangle the contributions of these two sources of noise in the fluctuations. With this method we will therefore be able to compute χ_{th} and the sum of $\chi_{het} + \chi_{dis}$ but not each term separately. Since we expect the contribution due to the quenched disorder (χ_{dis}) to be small, we will improperly call χ_{het} the latter sum. Notice that, besides the choice of the random coupling J_μ, an additional source of quenched disorder comes from the choice of the random graph. It is known, however, that local properties of random regular graphs are self-averaging and consequently the effect of topology fluctuations are even smaller.

We have simulated at the dynamical critical temperature T_d systems of size ranging from $N = 150$ to $N = 2400$, with a number of samples N_S such that $N \times N_S = 3.7 \cdot 10^7$. In order to be able to measure both χ_{th} and χ_{het}, for each sample $\alpha = 1, \ldots, N_S$ we have simulated two independent trajectories $s = 1, 2$ starting from the same equilibrium configuration and evolving with different thermal noises. Then for each sample and each trajectory we measure the correlation functions $C_{\alpha,s}(t) = \frac{1}{N}\sum_i S_i^\alpha(0) S_i^{\alpha,s}(t)$, where the initial state is equal for the two trajectories. The susceptibilities are then estimated as

$$\chi_{th} = \frac{1}{2N_S}\sum_{\alpha,s}(C^{\alpha,s})^2 - \frac{1}{N_S}\sum_{\alpha,s} C^{\alpha,1}C^{\alpha,2}, \tag{84}$$

$$\chi_{het} = \frac{1}{N_S}\sum_{\alpha,s} C^{\alpha,1}C^{\alpha,2} - \left(\frac{1}{2N_S}\sum_{\alpha,s}(C^{\alpha,s})\right)^2. \tag{85}$$

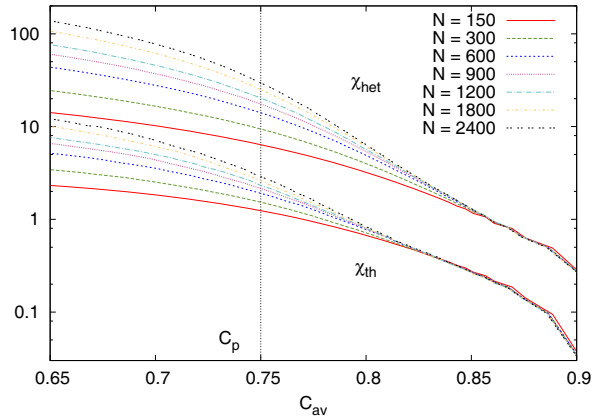

Fig. 3. Thermal susceptibility χ_{th} (lower data) and heterogeneity susceptibility χ_{het} (upper data) *versus* average correlation C_{av} for the 3-spin gauged model. The vertical line marks the analytical value of C_p.

These susceptibilities are shown in fig. 3. The very large number of samples simulated allows to reduce the statistical noise and to work on very clean data. We notice that for large values of C_{av} the data converge, as expected, to a finite value in the $N \to \infty$ limit: in this regime, dynamical fluctuations due to heterogeneities are roughly one order of magnitude larger than those due to thermal noise.

We now check finite size scaling of χ_{th} and χ_{het}, which, for $\epsilon = 0$, read

$$\chi_{th}(\phi, 0, N) = N^{1/4}\, h_{th}(\phi N^{1/4}), \tag{86}$$

$$\chi_{het}(\phi, 0, N) = N^{1/2}\, h_{het}(\phi N^{1/4}). \tag{87}$$

In fig. 4 we plot the rescaled susceptibilities, $\chi_{th}N^{-1/4}$ and $\chi_{het}N^{-1/2}$, as a function of $\phi = C_{av} - C_p$ for various values of N. We see that, in agreement with the analytical predictions, the different curves cross very close to $C = C_p = 0.75$. A more detailed analysis confirms that the crossing point tends to C_p for large N.

Before testing the $\phi N^{-1/4}$ scaling, we want to discuss the main source of finite size effects in the gauged model. By choosing the coupling signs independently, we have that energy fluctuations in the initial configuration are $O(N^{-1/2})$, but with a rather large coefficient if compared to the thermalized symmetric model. The main consequence is that, even for $N = O(10^3)$, the vast majority of samples have either an initial energy much larger than $E_d \equiv -z/3 \tanh(1/T_d)$ (and thus decorrelate very fast), either much smaller than E_d (and thus are stuck at $C > C_p$). The final effect is to have larger fluctuations and larger finite size effects, with respect to a model where the initial energy is more concentrated around E_d. Given that, in the thermodynamical limit, the energy must converge to E_d, we introduce a new *fixed-energy* model where the initial energy is fixed to E_d. This is achieved generating samples with a fixed number of negative coupling equal to $M(1 - \tanh 1/T_d)/2$.

We have simulated the fixed-energy model for sizes ranging from $N = 300$ to $N = 2400$, with 2 thermal histories per sample and a number of samples N_S such that $N \times N_S = 3 \cdot 10^7$. In the main panels of figs. 5 and 6 we show the rescaled susceptibilities $\chi_{th}N^{-1/4}$ and $\chi_{het}N^{-1/2}$ as a function of the average correlation for several system sizes. A comparison to the gauged model (see fig. 4) shows that finite size effects are reduced in this new model: indeed in figs. 5 and 6 data cross exactly at $C_{av} = C_p$ with almost no finite size corrections.

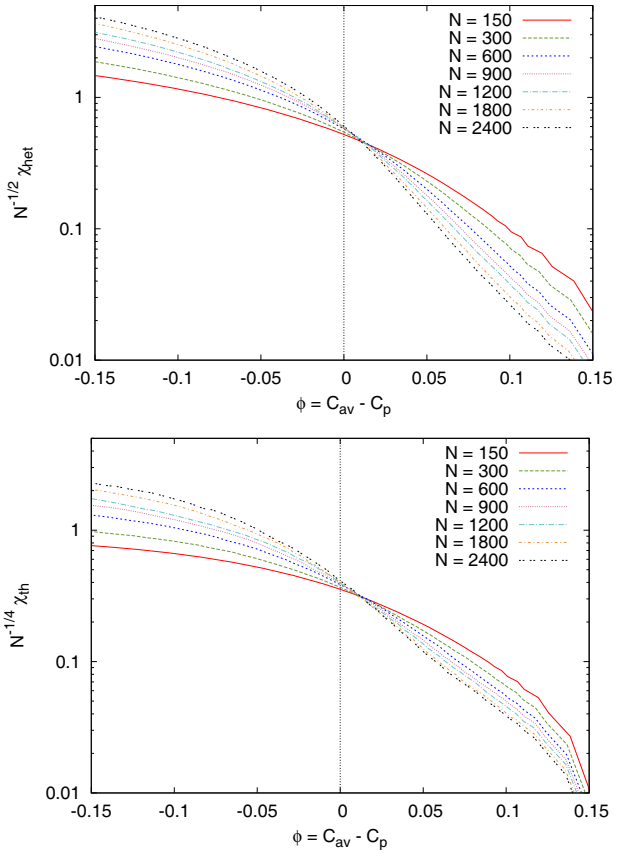

Fig. 4. Rescaled heterogeneity susceptibility χ_{het} (top) and thermal susceptibility χ_{th} (bottom) in the gauged 3-spin model discussed in the text at the dynamical critical temperature T_d as a function of the average correlation C_{av} for several sizes. The crossing point moves towards $C_{av} = C_p$ (marked by a vertical line) for large N.

We test then the $\phi N^{-1/4}$ scaling in the insets of figs. 5 and 6, where the same rescaled susceptibilities are plotted now as a function of the scaling variable $N^{-1/4}(C_{av} - C_p)$. We note that a good scaling is observed in a relatively wide region around the origin.

In fig. 7 we show, as a function of C_{av}, the ρ ratio defined in eq. (39), which, for $k = 0$, is

$$\rho = \frac{\chi_{het}}{\chi_{th}^2}\,. \tag{88}$$

As expected, the curves cross at C_p. The limit $\lim_{C \to C_p} \lim_{N \to \infty} \rho(\phi, N)$ taken in the specified order, is a direct measure of the variance of the random temperature entering the field theory, $-(m_2 + m_3)$. Unfortunately the

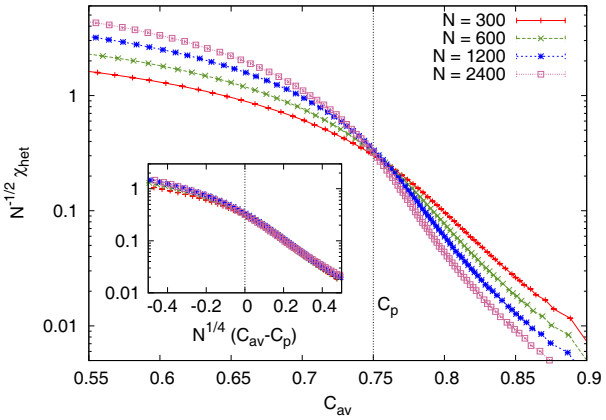

Fig. 5. Scaled heterogeneity susceptibility $\chi_{het}N^{-1/2}$ in the fixed-energy 3-spin model.

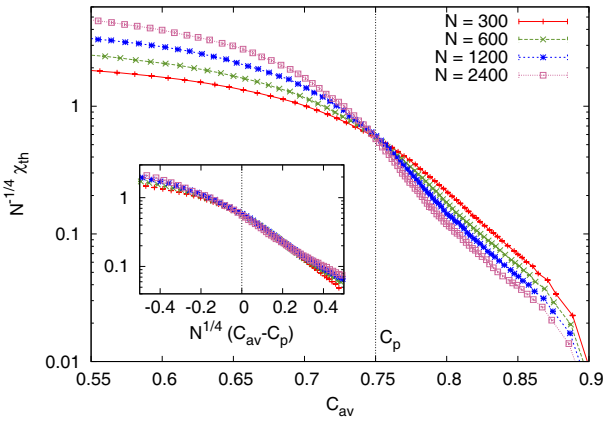

Fig. 6. Scaled thermal susceptibility $\chi_{het}N^{-1/4}$ in the fixed-energy 3-spin model.

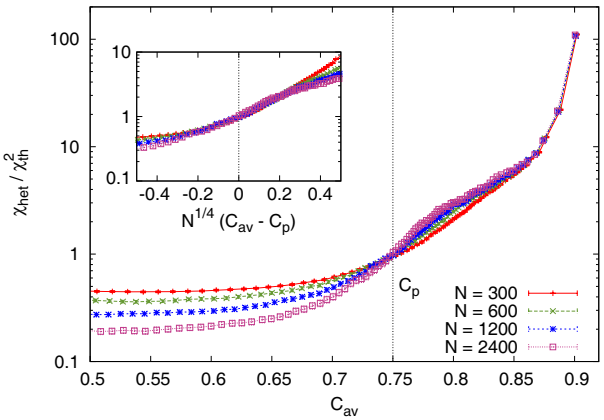

Fig. 7. Plot of the susceptibility ratio $\rho = \chi_{het}/\chi_{th}^2$ as a function of C_{av}. The curves cross in C_p, where, as seen in the inset, the slope scales as $N^{1/4}$.

values of N we can simulate do not allow an estimate of this limit. However we can see the scaling of slope $\mathrm{d}\rho/\mathrm{d}C$ in C_p which behaves as $N^{1/4}$, which confirms the formation of a discontinuity.

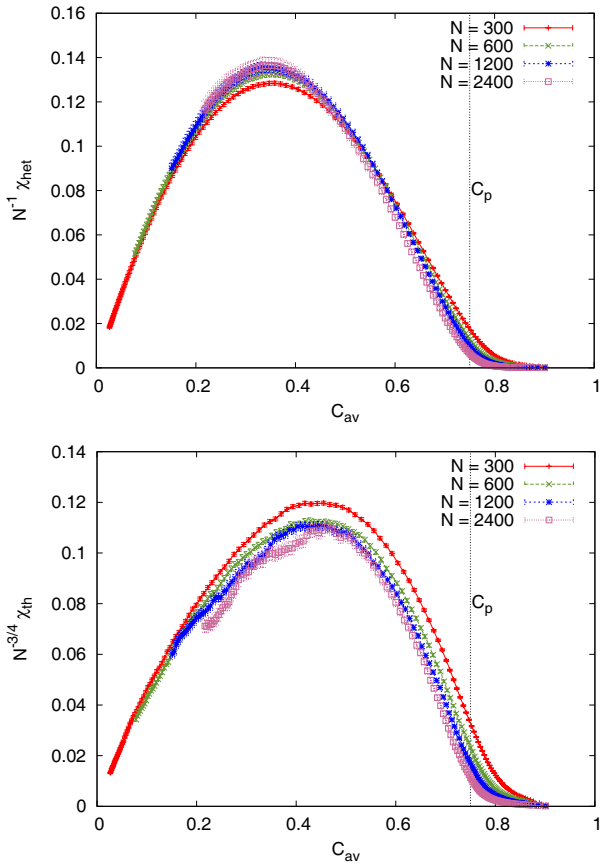

Fig. 8. Rescaled $N^{-1}\chi_{het}$ (top) and $N^{-3/4}\chi_{th}$ (bottom) in the alpha regime.

7.2 Simulations in the alpha regime

In order to study fluctuations in the alpha regime, the use of the fixed-energy model is mandatory. Indeed the finite size effects in the gauged model described above (strong fluctuations in the initial configuration energy) amplify in the alpha regime, making the gauged model almost useless. The fixed-energy model, on the contrary, produces data showing a much better scaling.

First of all we note that the different scaling between fluctuations due to heterogeneities and those due to thermal noise persists in the alpha regime. Indeed χ_{het} and χ_{th} show different size dependence even for $C_{av} < C_p$, as can be seen in fig. 8. While the scaling of χ_{het} is clearly $O(N)$, that of χ_{th} has a smaller power: the data shown in fig. 8 (bottom) suggest the value 3/4 argued for in sect. 6.2 to be an upper bound to the right power.

In fig. 9 we report data for the rescaled total susceptibility χ_4/N as a function of the average correlation. The qualitative behaviour seems to reflect quite well the bistable behaviour discussed in sect. 6, and represented in fig. 9 with the parabola $C_{av}(C_p - C_{av})$. However some deviations from this behavior are expected, especially for C_{av} close to C_p, because the time to relax from C_p to 0 is comparable to the time for entering the alpha regime in the fastest samples: as explained, the final result should be that χ_4/N is quadratic around C_p.

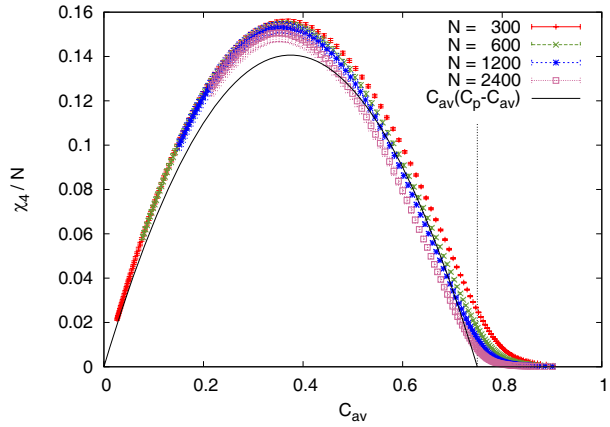

Fig. 9. Plot of the total rescaled susceptibility χ_4/N as a function of C_{av} in the alpha regime. The curves for different values of N are compared with the parabola $C_{av}(C_p - C_{av})$, derived under the hypothesis of a perfect bistability relaxation process.

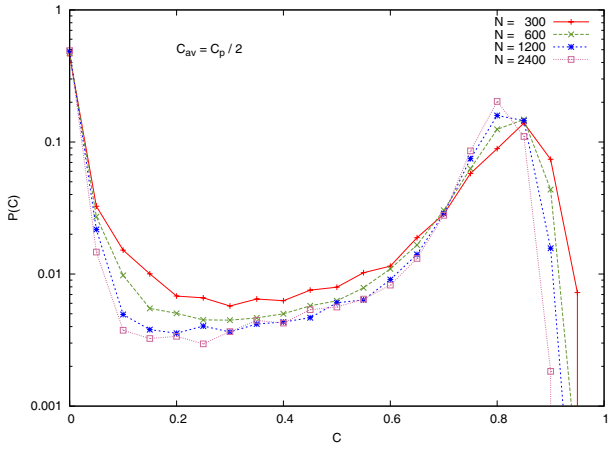

Fig. 10. Histogram of the correlation for $C_{av} = C_p/2$ on a logarithmic scale. While the data clearly show a bistable behavior, still a non-vanishing part of the distribution between the two peaks seems to persists for large N.

Bistability can be checked directly by looking at the histogram of correlations. In fig. 10 we report such histograms measured at times such that the mean correlation satisfies $C_{av} = C_p/2$; this time grows with system size. The shape of the histograms in fig. 10 is clearly made of two well-separated peaks. However one may notice that there is a small but non-zero probability (apparently not vanishing when $N \to \infty$) of finding intermediate values of correlation, and this is another plausible explanation for the deviations of χ_4/N from the predicted parabola $C_{av}(C_p - C_{av})$.

8 Concluding remarks

In this paper we emphasize the importance of describing fluctuations in a reparameterization-invariant form in glassy systems. We provide a universal theory of these fluctuations in the beta regime close to the mode coupling transition.

There are three main physical ingredients in our theory:

1) Time scale separation, leading to quasi-equilibrium sampling of metastable states.
2) The vicinity to a dynamical critical point.
3) Neglection of all possible non-perturbative effects.

The first property allows us to study fluctuations through the use of constrained equilibrium measures and their associated glassy effective potential. These measures depend on a reference configuration which is itself randomly chosen with canonical distribution. In this paper we have extended the theory of the effective potential to study fluctuation with respect to this source of noise. We have considered the effective potential for fixed initial configuration as a random functional whose probability distribution relates to the one of overlap fluctuations and therefore to dynamical heterogeneities. In our description time is eliminated and we use the average correlation function as a clock.

The second property allows us to invoke universality and to use the general form of replica field theory that can be obtained by symmetry considerations as an expansion around a Mode Coupling Transition point. The analysis of this theory leads to the identification of the relevant fluctuation modes. The effective field theory that describes them reduces, through tremendous simplifications, to a scalar cubic field theory with a local random field term. The random field term is the expression of heterogeneity in the initial condition and acts as a source of disorder that influences the subsequent dynamics. A remarkable consequence of our description is that fluctuations with respect to different sources of noise show different singular behavior as the dynamic transition is approached.

The third point is quite delicate. In deriving the equivalence with the RFIM, all barrier jumping processes are neglected. Quite naturally one could hypothesize validity of the RFIM description beyond perturbation theory. However, the dynamics in the non-perturbative region, even its reparametrization-invariant part, could be very different in the RFIM and in supercooled liquids. The analogy between liquid dynamics and the decay of metastable phases decay is only partially valid. In ordinary first-order transition kinetics, competition between interface and volume free energy leads to fast growth of supercritical nuclei. This fast growth should not be present in supercooled liquids.

We tested our scenario in the favourable case of finite size scaling in mean-field models. More work will be needed to test the scenario in liquid models. In low dimension the critical—or pseudocritical—properties of the spinodal point of RFIM can hardly be computed analytically. One should therefore compare numerical results of simulations of liquids with numerical results on the RFIM, however the situation might be complicated by the fact that non-perturbative effects could be different in the two kinds of systems.

An important prediction of our theory is that the different components of the dynamical fluctuations have different scaling properties. Within a Gaussian approximation we have found that the heterogeneous susceptibility is proportional to the square of the thermal one. It is not clear to us if this simple quadratic relation holds beyond the Gaussian approximation or two non-simply related exponents describe the corresponding singularities. This is an important point that will need to be clarified through numerical simulations.

We thank H. Castillo and G. Tarjus for discussions. SF acknowledges the hospitality of the Dipartimento di Fisica, Sapienza Università di Roma.

References

1. L. Berthier, G. Biroli, J.-P. Bouchaud, L. Cipelletti, W. van Saarloos (Editors), *Dynamical Heterogeneity in Glasses, Colloids and Granular Media* (Oxford University Press, 2011).
2. S. Das, Rev. Mod. Phys. **76**, 785 (2004) (for a review of mode coopling theory).
3. D.R. Reichman, P. Charbonneau, J. Stat. Mech. P05013 (2005) (for a review of mode coopling theory).
4. S. Franz, G. Parisi, J. Phys.: Condens. Matter **12**, 6335 (2000).
5. C. Donati, S. Franz, G. Parisi, S.C. Glotzer, J. Non-Cryst. Solids **307-310**, 215 (2002).
6. J. Bouchaud, G. Biroli, Europhys. Lett. **67**, 21 (2004).
7. For a review see P. Harrowell *The lengthscales of dynamic heterogeneity: results from molecular dynamics simulations*, Chapt. 7 in [1].
8. L. Berthier, G. Biroli, J.-P. Bouchaud, L. Cipelletti, D. El Masri, D. L'Hote, F. Ladieu, M. Pierno, Science **310**, 1797 (2005) See R. Riechert *et al.*, Chapt. 5 of [1] for a review.
9. Reviews of the Random First Order Theory can be found in V. Lubchenko, P.G. Wolynes, Annu. Rev. Phys. Chem. **58**, 235 (2006), and G. Biroli, J.P. Bouchaud, "The Random First-Order Transition Theory of Glasses: a critical assessment" arXiv:0912.2542.
10. S. Franz, G. Parisi, J. Phys. I **5**, 1401 (1995).
11. S. Franz, G. Parisi, Phys. Rev. Lett. **79**, 2486 (1997).
12. S. Franz, G. Parisi, Physica A **261**, 317 (1998).
13. L.F. Cugliandolo, J. Kurchan, Phys. Rev. Lett. **71**, 173 (1993).
14. L.F. Cugliandolo, J. Kurchan, J. Phys. A: Math. Gen. **27**, 5749 (1994).
15. L. Berthier, G. Biroli, J.-P. Bouchaud, W. Kob, K. Miyazaki, D. Reichman, J. Chem. Phys. **123**, 184503 (2007) and 184504.
16. C. Chamon, M. Kennett, H. Castillo, L.F. Cugliandolo, Phys. Rev. Lett. **89**, 217201 (2002).
17. H. Castillo, C. Chamon, L.F. Cugliandolo, J.L. Iguain, M.P. Kennett, Phys. Rev. B **68**, 134442 (2003).
18. C. Chamon, L.F. Cugliandolo, J. Stat. Mech. P07022 (2007).
19. K.E. Avila, H.E. Castillo, A. Parsaeian, "Mapping dynamical heterogeneity in structural glasses to correlated fluctuations of the time variables" arXiv:1007.0520.
20. For a review, see T. Nattermann, *Spin Glasses and Random Fields* (World scientific, Singapore, 1998) p. 277.
21. S. Franz, F. Ricci-Tersenghi, T. Rizzo, G. Parisi, *Properties of the perturbative expansion around the mode-coupling dynamical transition in glasses*, arXiv:1001.1746 (unpublished); *Critical behaviour of large scale dynamical heterogeneities in glasses: a complete theory*, arXiv:1008.0996, Proceedings of *StatphysHK*, Hong-Kong, July 2010; *Replica Field Theory of the Dynamical Transition in Glassy Systems*, arXiv:1105.5230 (submitted).
22. G. Parisi, J. Phys. A: Math. Gen. **30**, L765 (1997).
23. G. Parisi, J. Phys. Chem. B. **103**, 4128 (1999).
24. A. Widmer-Cooper, P. Harrowell, H. Fynewever, Phys. Rev. Lett. **93**, 135701 (2004).
25. A. Widmer-Cooper, P. Harrowell, J. Phys.: Condens. Matter **17**, S4025 (2005).
26. A. Widmer-Cooper, P. Harrowell, Phys. Rev. Lett. **96**, 185701 (2006).
27. A. Widmer-Cooper, P. Harrowell, J. Chem. Phys. **126**, 154503 (2007).
28. A. Widmer-Cooper, H. Perry, P. Harrowell, D.R. Reichman, Nat. Phys. **4**, 711 (2008).
29. C. Dasgupta, A. Indrani, S. Ramaswamy, M. Phani, Europhys. Lett. **15**, 307 (1991).
30. L. Berthier, R. Jack, Phys. Rev. E **76**, 041509 (2007).
31. G. Parisi, *On the probabilistic formulation of the replica approach to spin glasses*, cond-mat/9801081.
32. S. Franz, M. Mezard, G. Parisi, L. Peliti, J. Stat. Phys. **97**, 459 (1999).
33. S. Franz, R. Mulet, G. Parisi, Phys. Rev. E **65**, 021506 (2002).
34. J.-P. Bouchaud, M. Mezard, J. Phys. I **4**, 1109 (1994)); M. Mezard, G. Parisi, *Replicas and Glasses*, arXiv:0910.2838.
35. A. Andreanov, G. Biroli, J.-P. Bouchaud, EPL **88**, 16001 (2009).
36. G. Szamel, EPL **91**, 56004 (2010).
37. R. Monasson, Phys. Rev. Lett. **75**, 2847 (1995).
38. T. Temesvari, C. De Dominicis, I.R. Pimentel, Eur. Phys. J. B **25**, 361 (2002).
39. G. Parisi, N. Sourlas, Phys. Rev. Lett. **43**, 744 (1979).
40. M. Campellone, G. Parisi, P. Ranieri, Phys. Rev. B **59**, 1036 (1999).
41. J.R.L. de Almeida, D.J. Thouless, J. Phys. A: Math. Gen. **11**, 983 (1978).
42. J. Cardy, Phys. Lett. B **125**, 470 (1983).
43. J. Cardy, Physica D **15**, 123 (1985).
44. G. Parisi, N. Sourlas, Phys. Rev. Lett. **46**, 871 (1981).
45. M.E. Fisher, Phys. Rev. Lett. **40**, 1610 (1978).
46. C. Bagnuls, C. Bervillier, Phys. Rept. **348**, 91 (2001) (for a review).
47. G. Tarjus, M. Tissier, Phys. Rev. Lett. **93**, 267008 (2004).
48. M. Tissier, G. Tarjus, Phys. Rev. Lett. **96**, 087202 (2006).
49. T. Sarlat, A. Billoire, G. Biroli, J.-P. Bouchaud, J. Stat. Mech., P08014 (2009).
50. G. Biroli, private communication.
51. S. Karmakar, C. Dasgupta, S. Sastry, Proc. Natl. Acad. Sci. U.S.A. **106**, 3675 (2009).
52. J.S. Langer, Ann. Phys. (NY) **41**, 108 (1967).
53. F. Ricci-Tersenghi, A. Montanari, Phys. Rev. B **70**, 134406 (2004).
54. H. Nishimori, J. Phys. C: Solid State Phys. **13**, 4071 (1980)
55. G. Semerjian, A. Montanari, J. Stat. Phys. **124**, 103 (2006).
56. F. Krzakala, L. Zdeborova, J. Chem. Phys. **134**, 034512 (2011).
57. F. Krzakala, L. Zdeborova, J. Chem. Phys. **134**, 034513 (2011).